Available online at www.sciencedirect.com
SCIENCE DIRECT
Journal of the European Ceramic Society 26 (2006) 1273–1279
www.elsevier.com/locate/jeurceramsoc

Influence of the SiC grain size on the wear behaviour of Al_2O_3/SiC composites

M. Belmonte *, M.I. Nieto, M.I. Osendi, P. Miranzo

Instituto de Cerámica y Vidrio (CSIC), Campus de Cantoblanco, c/Kelsen 5, 28049 Madrid, Spain

Received 24 July 2004; received in revised form 22 December 2004; accepted 10 January 2005
Available online 3 March 2005

Abstract

Dry ceramic block-on-steel ring wear tests were performed at high loads in several Al_2O_3/20 vol.% SiC composites as a function of the SiC grain size, which ranged from 0.2 to 4.5 μm in d_{50}. The wear resistance of the monolithic alumina was radically improved by the addition of the SiC particles, reducing down to one order of magnitude wear rate. Two different behaviours were identified according to the microstructural observations on the worm surfaces: intergranular fracture and grain pull-out in the monolithic Al_2O_3, and plastic deformation and surface polishing in the composites. The wear resistance of the Al_2O_3/SiC composites increased with the SiC grain size due to their fracture toughness enhancement.

Keywords: Al_2O_3; SiC; Composites; Toughness and toughening; Wear resistance

1. Introduction

The success in improving either the mechanical or tribological properties of Al_2O_3 by adding SiC particles is very much influenced by their shape and size. For instance, fracture toughness, K_{IC}, of 9.5 MPa m$^{0.5}$ and flexural strength, σ, of 650 MPa, were measured for an Al_2O_3 based composite with 30 vol.% of SiC whiskers[1]—aspect ratios ranging from 20 to 160. Nevertheless, for the same volume fraction of SiC platelets – 17 μm of average size – a K_{IC} of just 7.0 MPa m$^{0.5}$ and a σ of about 400 MPa have been reported.[2] Furthermore, high σ, 1000 MPa, and relative low K_{IC}, 4.8 MPa m$^{0.5}$, have been reported for an Al_2O_3 composite with 5 vol.% of SiC nanoparticles[3] – 300 nm of mean particle size – although these data have not been reproduced by other authors.[4] These large differences in the mechanical properties seems to be related to variations in the fracture behaviour of the composites by the effect of the SiC particle size. It was observed that the fracture changed from intergranular in the composites containing coarse SiC particles to transgranular in the nanocomposites.[4,5]

The tribological properties of Al_2O_3 composites containing SiC whiskers, platelets or nanoparticles have been also studied,[6–15] although a comprehensive analysis of data reported in the literature is complicated, due to the wide gamut of test configurations and experimental parameters. As a general rule, the addition of SiC particles improves the wear resistance of the composites compared to that of the monolithic alumina as detailed below.

Yust et al.[6] performed self-mated dry pin-on-disc wear tests on Al_2O_3/SiC whisker composites, reporting a decrease in the wear rate of almost two orders of magnitude when SiC whiskers were added to an Al_2O_3 matrix. Liu et al.[7] found comparable results using a cylinder-on-cylinder configuration under lubrication where one of the cylinders was the ceramic composite and the other was carburized steel. Farmer et al.[8] carried out similar tests than those of Yust et al. though under more severe wear conditions. These authors showed that wear rates of the SiC whisker containing Al_2O_3 samples increased with temperature but they always remained about an order of magnitude below the wear rate of monolithic Al_2O_3.

* Corresponding author.
E-mail address: mbelmonte@icv.csic.es (M. Belmonte).

0955-2219/$ – see front matter © 2005 Elsevier Ltd. All rights reserved.
doi:10.1016/j.jeurceramsoc.2005.01.049

Some of the present authors have also analyzed[9] the influence of the SiC content in the wear behaviour of Al_2O_3/SiC-platelet composites. Unlubricated ceramic block-on-steel ring wear tests done at high loads evidenced that, for short sliding distances and platelet contents $\leq$12 vol.%, the wear volume of the composites was similar to that of the monolithic alumina. However, for higher platelet contents and longer sliding distances, the wear volume of the composite increased faster than that of the alumina specimen. This behaviour was explained by the existence of a triboelectrification mechanism and by the large size of the SiC platelets. As polarization occurs during wear tests, the presence of two phases with different electrical properties (as Al_2O_3 and SiC) leads to the storage of polarization energy at the grain boundaries, whose relaxation may produce the material dielectric breakdown.[9] Material volume removed by this phenomenon would increase with the grain size of either the dispersed particles or the matrix.

Davidge et al.[10] performed wet erosive wear tests in Al_2O_3/SiC nanocomposites. Adding SiC nanoparticles of $\sim$100 nm in size led to a significant reduction in the wear rate compared to that of monolithic alumina samples of equivalent grain size, the reduction factor being dependent on the matrix grain size. Using same wear test conditions, Sternitzke et al.[11] analyzed the effect of SiC nanoparticle size (from 12 to 115 nm) in the wear resistance of the Al_2O_3/SiC nanocomposites. The smaller sizes led to the more wear resistant composites due to a change in the fracture mode from brittle intergranular fracture to plastic deformation. Rodriguez et al.[13] carried out reciprocating ball-on-flat wear tests on Al_2O_3 and different Al_2O_3/SiC composites containing either submicron particles (800 nm) or nanoparticles (40 and 200 nm) of SiC. At high contact loads, the nanocomposites increased their wear resistance in two orders of magnitude referred to the base Al_2O_3, meanwhile the submicron SiC particles only increased its wear resistance by a factor of $\sim$5. Finally, Kara and Roberts[15] reported an improvement on the erosive wear resistance of Al_2O_3 by a factor of 2–3 just by adding 1% by volume of SiC nanoparticles.

Despite the number of works describing the wear behaviour of Al_2O_3/SiC composites, few of them pay attention to the effect of the SiC particle size itself, the majority being focused on the wear resistance improvement of the Al_2O_3. Moreover, due to the large variety of wear tests employed, the comparison of the results obtained by the different research groups is not straightforward. Therefore, the aim of the present work is to investigate the wear behaviour of Al_2O_3/20 vol.% SiC composites as a function of the SiC particle size, from 0.2 to 4.5 μm of mean particle size (d_{50}), using dry ceramic block-on-steel ring wear tests.

2. Experimental procedure

A submicronic α-Al_2O_3 powder (Alcoa CT-3000SG) with a mean particle size of 0.5 μm and four different SiC powders, with average grain sizes ranging from 0.2 to 4.5 μm, were selected as starting materials (see Table 1 for details). Each Al_2O_3/SiC powder mixture containing a 20 vol.% of the second phase was ball milled with Al_2O_3 grinding media in isopropyl alcohol during 75 min, dried at 60 °C and sieved by a 60 μm mesh. The homogeneous powder mixtures were hot pressed at 1500 °C for 30 min in argon atmosphere applying a uniaxial pressure of 50 MPa during the thermal cycle. A monolithic Al_2O_3 compact was obtained using the same hot pressing conditions for comparative purposes.

The Al_2O_3/SiC composites are labelled according to the SiC grain size as shown in Table 1: C means coarse, M medium (same as C powder but ball milled for 100 h), S submicron and N nanoparticles.

Final densities of the specimens were measured by the Archimedes' immersion technique in water. The microstructure was analyzed on polished and thermally etched, at 1400 °C in Ar atmosphere, samples by optical and scanning electron microscopy. The average matrix grain size was estimated on SEM micrographs using image analysis techniques and measuring at least 200 features for each specimen.

Table 1
Microstructural, mechanical and thermal data of the Al_2O_3/SiC composites (d_{50} = mean particle size; ρ = relative density; ρ_{th} = theoretical density; D = average matrix grain size; H = hardness; E = Young's modulus; K_{IC} = fracture toughness; κ = thermal conductivity)

	Al_2O_3[a]	SiC "C"[b]	SiC "M"[c]	SiC "S"[d]	SiC "N"[e]
d_{50} (μm)	0.5	4.5	1.7	0.8	0.2
ρ (g cm^{-3}) (% ρ_{th})	3.98 (99.9)	3.79 (99.2)	3.80 (99.5)	3.77 (98.7)	3.53 (92.4)
D (μm)	0.83 ± 0.52	0.86 ± 0.53	0.80 ± 0.51	0.44 ± 0.42	0.24 ± 0.16
H (GPa)	15.7 ± 0.6	18.0 ± 0.1	17.9 ± 0.3	18.8 ± 0.1	19.2 ± 0.4
E (GPa)	388 ± 3	403 ± 4	389 ± 3	394 ± 3	–
K_{IC} (MPa m$^{1/2}$)	4.3 ± 0.1	5.9 ± 0.3	5.2 ± 0.4	4.9 ± 0.2	3.0 ± 0.4
$\kappa_{25\,°C}$ (W m^{-1} K^{-1})	29.5 ± 1.5	31.0 ± 1.6	29.2 ± 1.5	27.4 ± 1.4	17.1 ± 0.9
$\kappa_{600\,°C}$ (W m^{-1} K^{-1})	10.7 ± 0.5	13.5 ± 0.7	12.8 ± 0.6	12.7 ± 0.6	9.3 ± 0.5

[a] Alcoa CT-3000SG, Germany.
[b] Navarro, Spain.
[c] Navarro milled for 100 h.
[d] Cerac S-2022, USA.
[e] Lonza UF45, Switzerland.

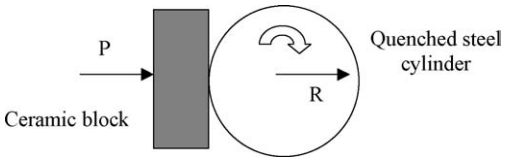

Fig. 1. Diagram of the wear test configuration.

The thermal conductivity (κ) of the Al_2O_3 compact and the Al_2O_3/SiC composites was calculated from the thermal diffusivity data (α) measured by the laser flash method using the methodology described elsewhere.[16]

The mechanical characterization of the composites included the measurements of the hardness (H), the Young's modulus (E) and the fracture toughness (K_{IC}). The hardness was determined by Vickers indentation tests using a load of 98 N. The dynamic Young's modulus was measured by the impulse excitation technique on prismatic bars of dimensions 3 mm × 4 mm × 40 mm. The fracture toughness was assessed by the single edge V-notched beam method in prismatic bars of 6 mm × 4 mm × 40 mm, each bar was centre notched to less than one-half its thickness and tested in 3-point bending using 30 mm of span.

Dry sliding wear tests were carried out using a block-on-ring tribotester, being the ring a quenched steel cylinder (0.35% C and 1% Cr) of 35 mm diameter and 50 HRC hardness, which rotated against the ceramic block (10 mm × 10 mm × 5 mm). Fig. 1 illustrates the wear test configuration. The ceramic testing surfaces were previously polished to achieve a roughness below 0.06 μm. The experiments were done at a constant load of 700 N with a rotational speed of the ring of 200 rpm, which corresponds to a linear velocity of 0.36 m s^{-1}, keeping its tolerance to the concentricity in the range of 0.02–0.04 mm. The tests were conducted in air at three different sliding distances: 650, 1300 and 2600 m. The wear volume (W_V) was determined using the following equation according to the wear track dimensions:

$$W_V = L\left[R^2 \arcsin\left(\frac{b}{2R}\right) - \frac{b}{4}\sqrt{(4R^2 - b^2)}\right] \quad (1)$$

where b and L are the width and the length, respectively, of the wear track, R is the radius of the cylinder and $b/2R$ must be expressed in radians. The wear coefficient (W_C) was calculated dividing the wear volume by the applied load (P); and the wear rate (W_R) was estimated dividing W_C by the sliding distance (x). Wear track parameters were measured on SEM micrographs once the wear debris was removed by etching with diluted HCl. Microstructure of the wear tracks and the debris were analysed by SEM–X-ray energy dispersive spectroscopy (EDS).

3. Results

The microstructures of the monolithic Al_2O_3 and the four Al_2O_3/SiC composites are shown in Figs. 2 and 3, respectively. The SiC particles in the composites are easily distinguished by their smoother surface, especially in the case of the C composite with the largest SiC particles (Fig. 3a). It can be observed how the Al_2O_3 grains protrude form the surface due to the thermal etching. For the C and M specimens, the grain sizes are similar and comparable to the monolithic alumina (∼0.8 μm) but bigger than for the S and N composites (0.44 and 0.24 μm, respectively), as Table 1 summarized. S and N composites also show lower densities.

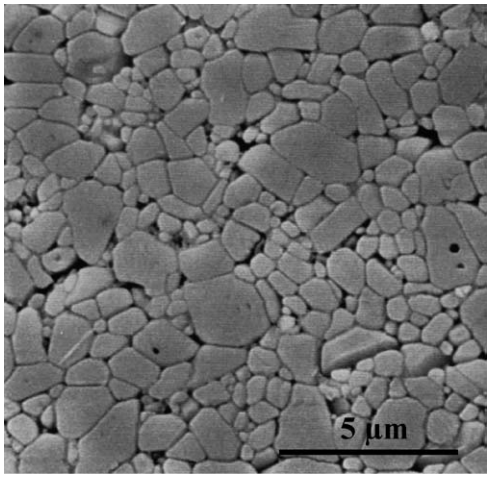

Fig. 2. SEM micrograph of the monolithic Al_2O_3 specimen after polishing and etching at 1400 °C/0 min in Ar atmosphere.

The wear coefficient as a function of the sliding distance is plotted in Fig. 4 for all the specimens. Different trends in the wear behaviour are observed for monolithic and composite materials. W_C for the Al_2O_3 compact increases up to one order of magnitude at the larger sliding distance tested, whilst it does not change for the C specimen and it only shows a slight increase for the M and S specimens. Among the composites, only the porous N specimen evidences a large augment on W_C.

The formation of an almost continuous film, the so-called third body, has been observed for all the materials after wear tests. In all the materials, this film shows similar appearance and an example is given in Fig. 5. EDS analysis of these films proved the existence of a substantial amount of Fe.

The wear tracks for the Al_2O_3 and Al_2O_3/SiC specimens, once the third body is removed, have quite different microstructural features. The monolithic specimen shows evidence of intergranular fracture for all the sliding distances (see Fig. 6a and b). Conversely, the dense composites present smooth surfaces with indication of plastic deformation. As an example, the worn surfaces of the C composite for the wear tests performed at 1300 and 2600 m are shown in Fig. 6c and d, respectively. Similar features (Fig. 7) are observed for the nanocomposite, N, especially at 2600 m, with deep grooves and some evidence of fracture.

One main observation emerges when the wear rate is depicted versus SiC particle size, just for the largest sliding distance (Fig. 8): the wear rate decreases drastically by adding

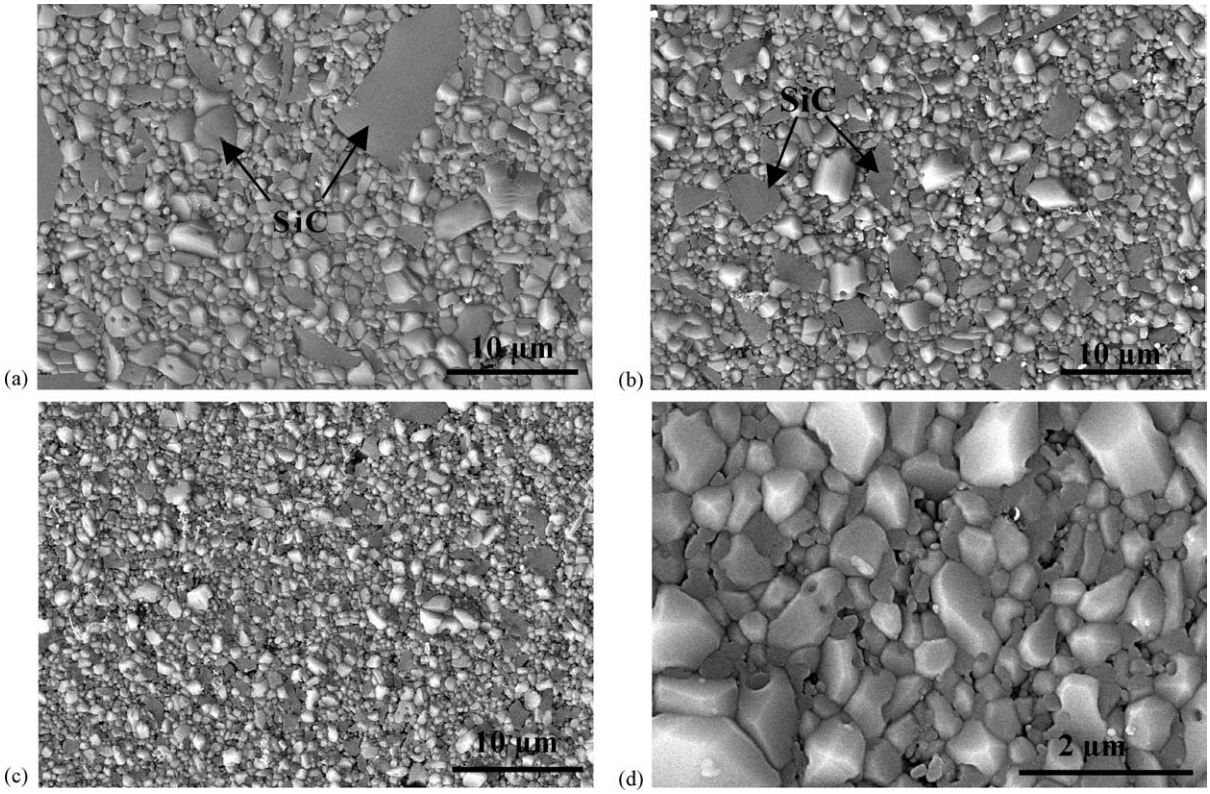

Fig. 3. SEM micrographs of the (a) C, (b) M, (c) S and (d) N composites, after polishing and etching at 1400 °C/10 min in Ar atmosphere.

SiC particles. Even more, W_R decreases as the SiC particle size increments.

4. Discussion

The microstructure of the materials, summarized in Table 1, can be explained using the sintering model proposed by Sundaresan and Aksay.[17] This model assumes an ideal composite with non-sinterable spheres, predicting a reduction in the sintering rate when the inter-inclusion distance decreases. For a given volume fraction of inclusions, this distance decreases as the inclusion size diminishes, which explains the observed falls in density and matrix grain size for small SiC grain sizes (composites S and N).

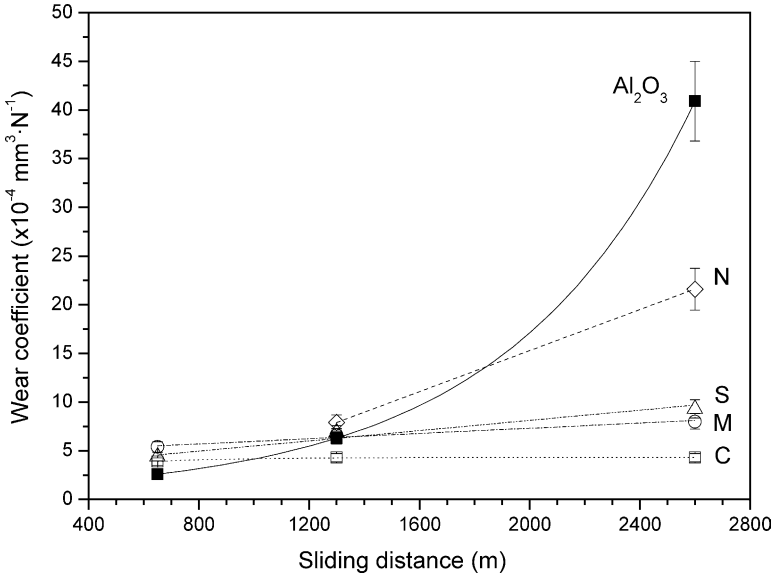

Fig. 4. Wear coefficient as a function of sliding distance for the monolithic Al_2O_3 specimen and the four Al_2O_3/SiC composites.

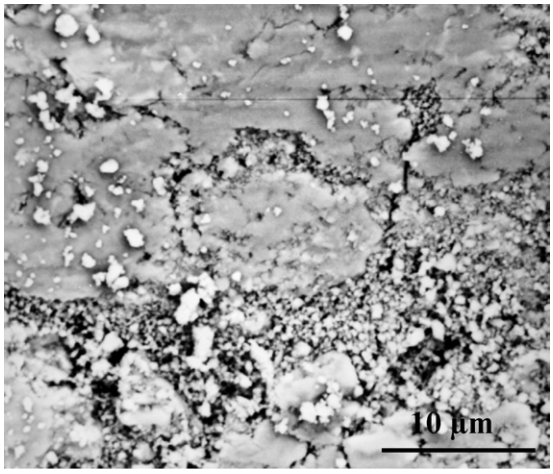

Fig. 5. SEM micrograph of the third body film developed on the N composite surface during the wear tests at 650 m of sliding distance.

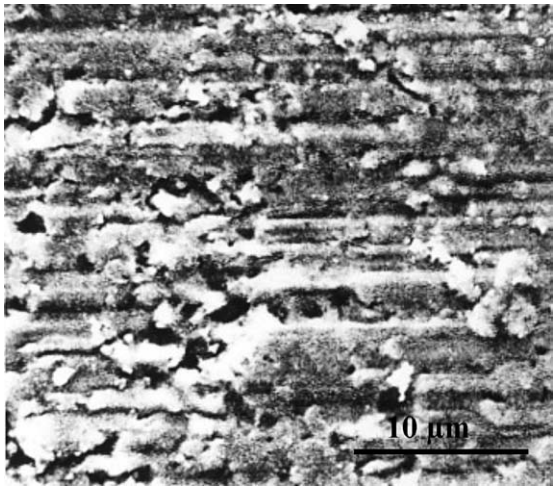

Fig. 7. SEM micrograph of the clean wear track for N specimen, after 2600 m of sliding distance.

The composites M and C, and the monolithic alumina have quite similar densities and matrix grain sizes (Table 1), and that allows the comparison of their wear responses. When considering the S composite, it should be taken into account that it presents alike density (~99% ρ_{th}) but a matrix grain size approximately one half of the values measured for the M and C composites.

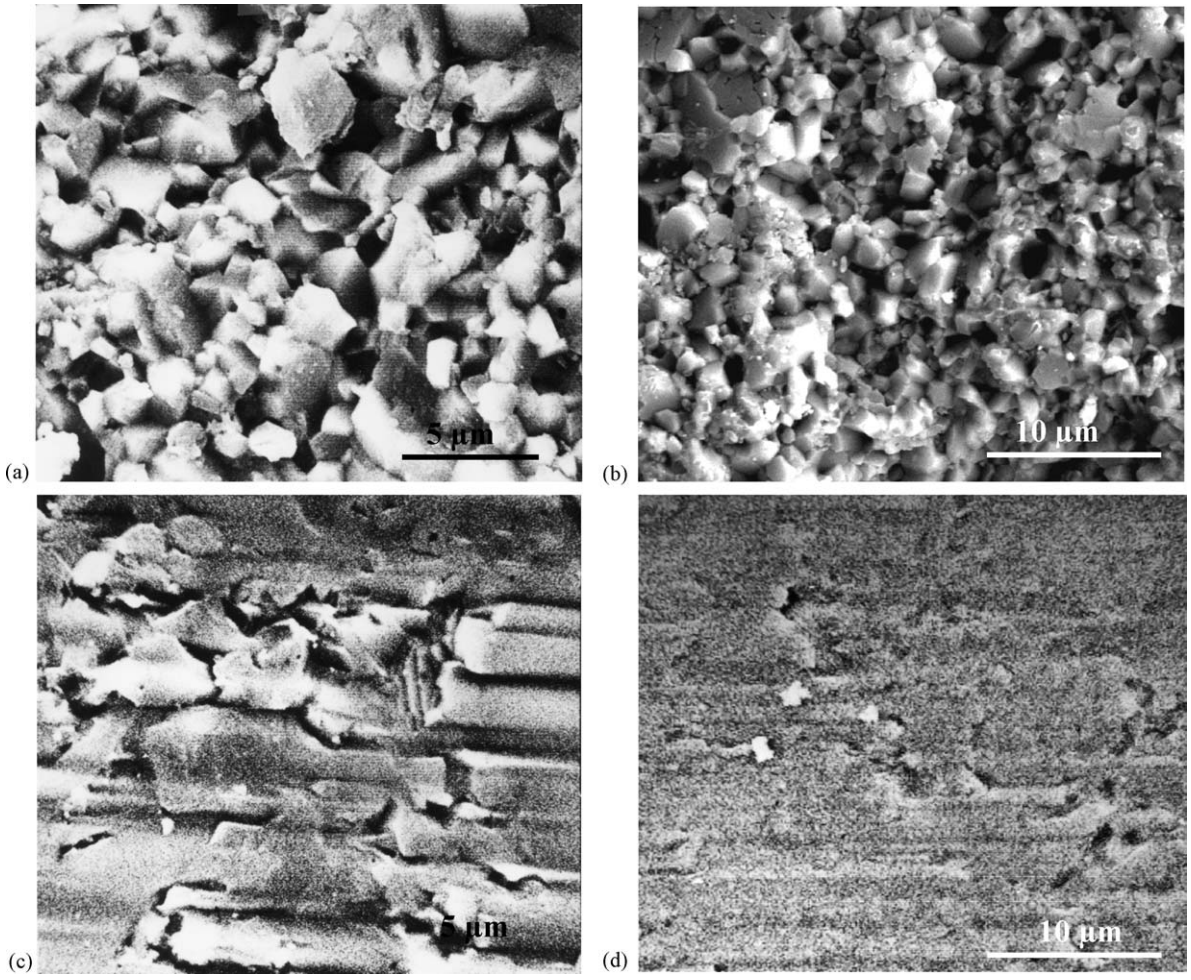

Fig. 6. SEM micrographs of the clean wear tracks for (a) monolithic Al_2O_3 (x = 1300 m), (b) monolithic Al_2O_3 (x = 2600 m), (c) C specimen (x = 1300 m) and (d) C specimen (x = 2600 m).

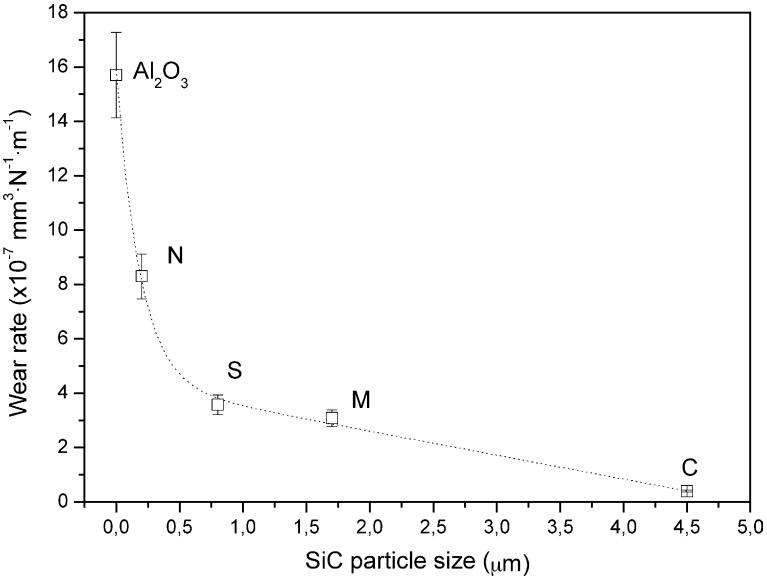

Fig. 8. Wear rate vs. the SiC particle size at 2600 m of sliding distance.

At sliding distances ≤1300 m, only small differences in wear coefficients were observed (Fig. 4). However, significant variations in the wear behaviour of the different materials were observed for longer sliding distance (x = 2600 m), which indicates that distinct wear mechanisms are occurring. This assumption is confirmed by the microstructural study of the worn surfaces (Fig. 6b and d). In this way, the W_C of the monolithic alumina shows an exponential growth with the sliding distance (Fig. 4), the main wear mechanism being intergranular grain boundary fracture and grain pull-out, as it can be observed in Fig. 6b. Therefore, a severe wear takes place in this material. On the other hand, W_C remains almost constant for the SiC containing alumina composites, exception made of the porous one (N). For these materials, wear tracks show less severe wear mode, where plastic deformation and surface polishing are the preferred wear mechanisms (Fig. 6d). The N composite presents a combined wear mode mixing plastic deformation and fracture, leading to pronounced groove formation and grain pull-out (Fig. 7).

The influence of the mechanical properties and the thermal residual stresses on the wear behaviour seems to be determinant in the materials. During the friction process, microcracks develop in the specimens due to surface fatigue and thus the higher fracture toughness of C, M and S materials will limit the crack propagation and the material removal compared to the Al_2O_3 with lower K_{IC} (Table 1). Moreover, SiC grains are under compressive stresses due to the mismatch in the thermal expansion coefficients of both Al_2O_3 and SiC,[18] which

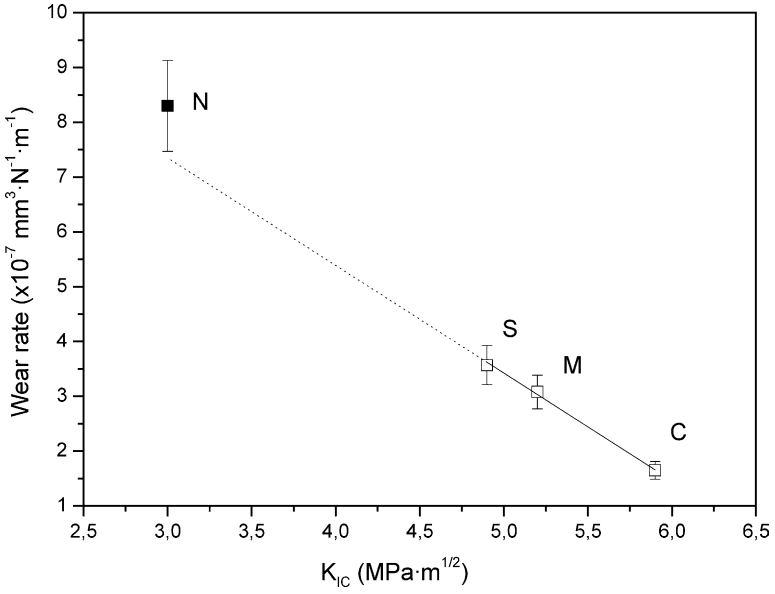

Fig. 9. Wear rate, W_R, at x = 2600 m as a function of fracture toughness, K_{IC}, for the Al_2O_3/SiC composites.

would reduce pull-out during friction processes. The later is also valid for the N composite although this material presents very low toughness and high wear rate due to its reduced density.

The dependence of the wear rate with the SiC grain size at $x = 2600$ m, shown in Fig. 8, could be also related to the mechanical properties and, to a lesser extent, to their thermal properties. Apart from the N composite, which has very low thermal conductivity, significant differences in κ values (see Table 1) were not observed neither at room temperature nor at 600 °C—approximately the surface temperature reached during the wear test.[9] Therefore, the fracture toughness is the key parameter that controls the wear behaviour of these composites, as the W_R versus K_{IC} plot evidences (Fig. 9).

Accordingly, W_R diminishes linearly with the fracture toughness for the dense composites, being the C composite, with a K_{IC} value of 5.9 MPa $m^{1/2}$, the most wear resistant ($W_R = 1.65 \times 10^{-7}$ mm^3 N^{-1} m^{-1}). The wear rate data of the *N* composite does not agree with this lineal fit and its high value is altered by its lower density. On the other hand, the matrix grain size does not seem to affect significantly the wear behaviour of these materials; comparing C and M composites, which have the same matrix grain size, an increase in K_{IC} of 13% leads to a reduction of ~50% in W_R. Besides, differences in matrix grain size of 50% (M and S specimens) produces variations of only 14% in wear rates. It should be noticed that the lineal dependence of W_R on K_{IC} is steeper than that proposed by Evans and Wilshaw[19] – $K_{IC}{}^{-3/4}$ dependence – for abrasive wear.

5. Conclusions

The reduction in wear rate down to one order of magnitude by the addition of SiC particles – 20% by volume – to Al_2O_3 is due to a change in the main wear mechanism: from intergranular fracture to plastic deformation.

The effect of the SiC grain size becomes significant for long sliding distances. The wear rate decreases with the SiC grain size, the fracture toughness being the key parameter that governs the wear behaviour of the composites. A lineal fit was established for the dense composites.

The sintering rate of Al_2O_3/SiC composites decreases with the SiC particle size due to a reduction in the inter-inclusion distance, which leads to lower densities and smaller matrix grain sizes for composite with SiC particles sizes below 1 μm.

Acknowledgements

This work has been funded by *Consejeria de Educacion de la CAM* (Spain) under project 07N/0095/2002. M. Belmonte acknowledges the financial support of the *"Ramón y Cajal"* program (MEC, Spain). The authors thank Dr. D. Treheux (Ecole Centrale de Lyon, France) for assisting in wear tests.

References

1. Homeny, J., Vaughn, W. L. and Ferber, M. K., Processing and mechanical-properties of SiC-whisker-Al_2O_3-matrix composites. *Am. Ceram. Soc. Bull.*, 1987, **67**, 333–338.
2. Belmonte, M., Moya, J. S., Miranzo, P., Nguyen, D., Dubois, J. and Fantozzi, G., Fracture behavior of Al_2O_3/SiC-platelet composites. *J. Mater. Res.*, 1996, **11**, 2528–2535.
3. Niihara, K., New design concept of structural ceramics–ceramic nanocomposites. *J. Ceram. Soc. Jpn.*, 1991, **99**, 974–982.
4. Perez-Rigueiro, J., Pastor, J. Y., Llorca, J., Elices, M., Miranzo, P. and Moya, J. S., Revisiting the mechanical behavior of alumina/silicon carbide nanocomposites. *Acta Mater.*, 1998, **46**, 5399–5411.
5. Ferroni, L. P. and Pezzotti, G., Evidence for bulk residual stress strengthening in Al_2O_3/SiC nanocomposites. *J. Am. Ceram. Soc.*, 2002, **85**, 2033–2038.
6. Yust, C. S., Leitnaker, J. M. and Devore, C. E., Wear of an alumina–silicon carbide whisker composite. *Wear*, 1988, **122**, 151–164.
7. Liu, H., Fine, M. E. and Cheng, H. S., Tribological behaviour of SiC-whisker/Al_2O_3 composites against carburized 8620 steel in lubricated sliding. *J. Am. Ceram. Soc.*, 1991, **74**, 2224–2233.
8. Farmer, S. C., Dellacorte, C. and Book, P. O., Sliding wear of self-mated Al_2O_3–SiC whisker-reinforced composites at 23–1200 °C. *J. Mater. Sci.*, 1993, **28**, 1147–1154.
9. Belmonte, M., Jurado, J. R., Treheux, D. and Miranzo, P., Role of triboelectrification mechanism in the wear behaviour of Al_2O_3–SiC platelet composites. *Wear*, 1996, **199**, 54–59.
10. Davidge, R. W., Twigg, P. C. and Riley, F. L., Effects of silicon carbide nano-phase on the wet erosive wear of polycrystalline alumina. *J. Eur. Ceram. Soc.*, 1996, **16**, 799–802.
11. Sternitzke, M., Dupas, E., Twigg, P. and Derby, B., Surface mechanical properties of alumina matrix nanocomposites. *Acta Mater.*, 1997, **45**, 3963–3973.
12. Lawrence, C. W., Wu, H. Z., Franco Jr., A., Roberts, S. G. and Derby, B., Erosion resistance of hot pressed Al_2O_3/SiC nanocomposites. *Sil. Ind.*, 1998, **63**, 73–75.
13. Rodriguez, J., Martin, A., Pastor, J. Y., Llorca, J., Bartolome, J. F. and Moya, J. S., Sliding wear of alumina/silicon carbide nanocomposites. *J. Am. Ceram. Soc.*, 1999, **82**, 2252–2254.
14. Lim, D. S., Park, D. S., Han, B. D., Kan, T. S. and Jang, H., Temperature effects on the tribological behaviour of alumina reinforced with unidirectionally oriented SiC whiskers. *Wear*, 2001, **251**, 1452–1458.
15. Kara, H. and Roberts, S. G., Wet erosion behaviour of low SiC alumina–SiC nanocomposites. *J. Mater. Sci.*, 2002, **37**, 2421–2426.
16. Barea, R., Belmonte, M., Osendi, M. I. and Miranzo, P., Thermal conductivity of Al_2O_3/SiC platelet composites. *J. Eur. Ceram. Soc.*, 2003, **23**, 1773–1778.
17. Sundaresan, S. and Aksay, I. A., Sintering with rigid inclusions-pair interactions. *J. Am. Ceram. Soc.*, 1990, **73**, 54–60.
18. Li, Z. and Bradt, R., Micromechanical stresses in SiC-reinforced Al_2O_3 composites. *J. Am. Ceram. Soc.*, 1989, **72**, 70–77.
19. Evans, A. G. and Wilshaw, T. R., Quasi-static solid particle damage in brittle solids. 1. Observations, analysis and implications. *Acta Metal*, 1976, **24**, 939–956.